Triptolide exerts antiviral effects and alleviates influenza A-induced pneumonia by inhibiting the overactivation of absent in melanoma 2 signaling in immune cells

YEYANG CHEN[1*], HUA WU[2*], XIANGJIAN WU[3*], LIKUN CHE[2], XIAOYAN FU[3], RUIHAN QI[3], DAN JIA[3], MINFANG LI[3], WEI XIE[3] and WENXIANG ZHU[3,4]

[1]School of Chinese Medicine, Hong Kong Baptist University, Hong Kong, SAR 999077, P.R. China; [2]School of Life Sciences, Beijing University of Chinese Medicine, Beijing 100029; P.R. China; [3]The Fourth Clinical Medical College, Guangzhou University of Chinese Medicine/Shenzhen Hospital of Traditional Chinese Medicine, Shenzhen, Guangdong 518033, P.R. China; [4]Nanozyme Laboratory in Zhongyuan, Henan Academy of Innovations in Medical Science, Zhengzhou, Henan 451163, P.R. China

Received April 11, 2025; Accepted August 5, 2025

DOI: 10.3892/ijmm.2026.5829

Abstract. Influenza A (H1N1) virus-induced pneumonia poses a significant clinical challenge because of excessive immune activation and limited targeted therapies. While current antivirals suppress viral replication, they fail to control absent in melanoma 2 (AIM2) inflammasome-mediated hyperinflammation, a key driver of immunopathology and mortality. The present study investigated whether triptolide (TP) ameliorates H1N1-induced pneumonia by targeting this unmet need. The results demonstrated that H1N1 infection reduced the levels of inflammatory cytokines in both human bronchial epithelial cells (HBEpiCs) and THP-1 cells and decreased the adhesion between the two cell types. Furthermore, high-dose H1N1 activation triggered the AIM2 signaling pathway in THP-1 cells but not in HBEpiCs and decreased the viability of THP-1 cells. *In vitro* and *in vivo* experiments both confirmed that TP effectively inhibited inflammation in alveolar epithelial cells and immune cells, as well as the adhesion between these cell types. Additionally, TP reduced the viral load of H1N1 in a murine pneumonia model. Further studies revealed that TP inactivated the AIM2 signaling pathway in THP-1 cells but not in HBEpiCs. However, overexpression of AIM2 in THP-1 cells markedly reversed the anti-inflammatory effects of TP. Based on these findings, it was hypothesized that TP modulates the immune response by inactivating the AIM2 signaling pathway in immune cells, which reduces excessive immune cell activation and decreases the harmful interactions between immune cells and alveolar epithelial cells, ultimately alleviating the lung inflammation induced by H1N1 virus infection. The present study proposed a novel mechanism by which TP alleviates lung damage by suppressing AIM2-driven immune hyperactivation in immune cells, thereby reducing harmful crosstalk with epithelial cells. This is the first evidence of AIM2-targeted therapy positioning TP as a promising candidate for treating viral pneumonia.

Correspondence to: Professor Wenxiang Zhu, Nanozyme Laboratory in Zhongyuan, Henan Academy of Innovations in Medical Science, Northeast Corner of Huanghai Road and Biotechnology Second Street, Zhengzhou Airport District, Zhengzhou, Henan 451163, P.R. China
E-mail: 2018011017@bucm.edu.cn

*Contributed equally

Key words: influenza A, pneumonia, absent in melanoma 2 signaling, immune cell, anti-virus

Introduction

Influenza A virus (IAV) surface antigens are highly prone to mutation, leading to the emergence of new subtypes (1). These mutations make it difficult for humans to effectively prevent influenza, thereby triggering large-scale outbreaks of influenza-like diseases (1). For instance, population-based hospitalization surveillance data from the United States demonstrates that H1N1pdm09 accounted for nearly one-quarter of laboratory-confirmed influenza-associated hospitalizations during the 2010-11 and 2018-19 influenza seasons (2). More critically, hospitalized patients with H1N1pdm09 infection exhibited a markedly elevated risk of developing severe outcomes, including ICU admission and in-hospital mortality, compared with those infected with H3N2 (2). The 2009 A/H1N1pdm09 pandemic led to the disappearance of the old seasonal A/H1N1. Since then we have had the COVID pandemic, so the way in which we approach airborne viruses has changed considerably. Importantly, not only A/H3N2 and B lineages but also A/H1N1pdm09 showed near-complete disappearance from global circulation during the COVID-19 pandemic, probably due to non-pharmaceutical interventions and behavioral changes (3). However, unlike B/Yamagata, A/H1N1pdm09 re-emerged after the relaxation of non-pharmaceutical interventions, highlighting its resilience and continued role in seasonal influenza dynamics. Upon IAV infection, the virus initially causes respiratory

tract infections, leading to congestion and edema of the upper respiratory mucosa and extensive epithelial cell shedding and necrosis (4). As the virus spreads, the lung tissue undergoes significant infiltration by inflammatory cells, with congestion, dilation, thickening and possible fusion of the alveolar walls (5). Additionally, bronchial epithelial cells may also undergo shedding and necrosis, ultimately resulting in lung tissue damage (5). In this process, the host immune response is often excessively activated, releasing large amounts of inflammatory cytokines such as interleukin (IL-)6, IL-10, tumor necrosis factor-α (TNF-α) and interferon-γ (IFN-γ) (6). The overproduction of these cytokines is one of the key pathological mechanisms underlying influenza virus-induced pneumonia. In particular, excessive production of TNF-α and IFN-γ not only activates a number of mononuclear macrophages but also exacerbates lung tissue damage (7). Although vaccination is the most effective method for preventing influenza, the efficacy of vaccines may gradually diminish due to viral mutations (7). Currently, drugs such as oseltamivir phosphate and amantadine are used to inhibit viral replication (8). However, a critical therapeutic gap persists: Although antiviral agents (such as the neuraminidase inhibitor oseltamivir and M2 inhibitors such as amantadine) can restrict viral replication, they are inadequate for modulating the dysregulated immune response of a host once systemic inflammation and cytokine storms are initiated (9,10). For example, studies have confirmed that while Tamiflu suppresses viral replication, its efficacy in regulating immune dysregulation (such as excessive release of TNF-α and IFN-γ) in patients with severe H1N1 pneumonia remains limited (11,12). Some patients continue to exhibit persistent viral replication and elevated inflammatory cytokine levels during treatment, demonstrating that single-agent antiviral therapy cannot halt disease progression. Consequently, there is an urgent need to shift therapeutic strategies from solely antiviral interventions to method for the comprehensive regulation of both viral replication and the host immune response, particularly by targeting the coexisting viral burden and excessive inflammation in patients with viral sepsis.

Innate immunity is the first line of defense against pathogen invasion, and inflammasome activation is a crucial component of the innate immune response (13). Absent in melanoma 2 (AIM2) is a cytosolic DNA sensor and a member of the PYHIN family that is capable of recognizing bacterial, viral, or host-derived cytosolic double-stranded DNA (13). Upon activation, AIM2 first recruits procaspase-1 through the adaptor protein ASC, leading to self-cleavage and activation of procaspase-1 (13). Activated caspase-1 then cleaves pro-IL-1β and pro-IL-18, generating mature IL-1β and IL-18, which are subsequently secreted extracellularly. Simultaneously, caspase-1 cleaves gasdermin D (GSDMD), producing the pore-forming N-terminal fragment GSDMD-NT, which forms pores in the cell membrane, inducing pyroptosis (14). This process regulates the inflammatory response and helps defend against pathogen infection and stress-induced damage. However, excessive activation of the AIM2 inflammasome may lead to an overly robust immune response, causing tissue damage and chronic inflammatory diseases (15). Under chronic inflammatory conditions, the sustained activation of AIM2 may contribute to the maintenance of chronic inflammation, increase the recruitment of immune cells, and promote the secretion of proinflammatory cytokines, ultimately leading to tissue damage and organ dysfunction (13). Therefore, modulating AIM2 activity may be a promising therapeutic strategy for treating various inflammatory diseases.

Triptolide (TP), the principal active component isolated from *Tripterygium wilfordii* (Celastraceae), exerts significant biological effects, including immunosuppressive, anti-inflammatory, antitumor and antifertility effects (16). A number of pharmacological and clinical studies have shown that TP plays a crucial role in regulating the immune system, particularly in inhibiting excessive immune responses and alleviating autoimmune diseases such as rheumatoid arthritis and nephritis (16-19). TP exerts its effects by targeting lymphocytes, inhibiting the overactivation of immune cells, and reducing immune-mediated inflammation, thereby improving disease symptoms and minimizing tissue damage (20). In the context of H1N1-induced pneumonia, viral infection typically triggers an exaggerated immune response, leading to the infiltration of inflammatory cells and the excessive release of inflammatory cytokines, such as IL-6 and TNF-α (21,22). This overactive immune response not only fails to effectively clear the virus but also exacerbates lung tissue damage, potentially leading to severe pneumonia and organ failure (21,22). Given the notable immunosuppressive and anti-inflammatory properties of TP, it was hypothesized that TP could specifically attenuate the dysregulated immune response and cytokine storm in H1N1 influenza-induced pneumonia, thereby reducing inflammatory lung damage and improving outcomes. Current therapies fail to concurrently address viral replication and dysregulated inflammation; however, the present study identified TP as a novel dual-function agent capable of both suppressing influenza virus proliferation and mitigating excessive host immune responses. Crucially, it revealed, for the first time to the best of the authors' knowledge, that TP exerts these effects by inhibiting the AIM2 inflammasome pathway, a key driver of pyroptosis and inflammation amplification in severe viral pneumonia.

Materials and methods

Cell culture. Immortalized human bronchial epithelial cells (HBEpiCs) were purchased from Shanghai Zhongqiao Xinzhou Biotechnology Co., Ltd. (cat. no. ZQ0001). The cell line was derived from normal bronchial epithelium obtained from a 54-year-old male patient who underwent lobectomy for squamous cell carcinoma. These cells were immortalized by infection with the recombinant retrovirus LXSN16E6E7, which carries the E6 and E7 genes of human papillomavirus type 16, followed by selection in medium containing 0.4 mg/ml G418. Consequently, these cells should be referred to as immortalized human bronchial epithelial cells rather than primary cells. These cells serve as a representative *in vitro* model for airway epithelial cells, which constitute the first line of defense against respiratory pathogens. The bronchial epithelium plays a pivotal role in mucociliary clearance and acts as a physical and immunological barrier, initiating innate immune responses upon pathogen invasion. THP-1 cells, a human monocytic cell line, obtained from Wuhan Procell Life Science

& Technology Co., Ltd., was derived from a patient with acute monocytic leukemia. THP-1 cells are widely used as models for human monocytes/macrophages in immunological studies because of their ability to differentiate into macrophage-like cells upon stimulation. They are instrumental in investigating monocyte/macrophage functions, signaling pathways, and inflammatory responses. HBEpiCs were cultured in bronchial epithelial cells complete culture medium (cat. no. ZQ-1322; Shanghai Zhongqiao Xinzhou Biotechnology Co., Ltd.), while THP-1 cells were cultured in RPMI-1640 supplemented with 10% fetal bovine serum (HyClone; Cytiva) and 1% penicillin-streptomycin (100X; Beijing Solarbio Science & Technology Co., Ltd.). All cultures were maintained at 37˚C in a humidified atmosphere with 5% CO_2.

The influenza A/PR/8/34 (H1N1) strain was obtained from the Pathogen Detection and Biosafety Laboratory of the Shanghai Public Health Clinical Center. The blank control group was treated with complete culture medium. The H1N1 virus infection group was infected with H1N1 virus at a multiplicity of infection (MOI) of 1.0 for 24 h to establish an HBEpiC model of H1N1 virus infection.

PMA induction. THP-1 cells ($1x10^6$ cells/ml) were seeded in a six-well plate and cultured for 24 h. Then, phorbol 12-myristate 13-acetate (PMA; MedChemExpress) was added to the culture medium at a final concentration of 100 nM. The cells were then incubated at 37˚C with 5% CO_2 for an additional 24 h to induce the differentiation of THP-1 cells into adherent macrophage-like cells.

TP intervention. After HBEpiCs were infected with H1N1 for 24 h, the cells were treated with various concentrations of TP (5, 10, or 20 nM; Beijing Solarbio Science & Technology Co., Ltd.) for an additional 24 h. Cell supernatants or cells were then collected for subsequent experiments.

Enzyme-linked immunosorbent assay (ELISA). Cell supernatants were collected and analyzed using Human TNF-α High Sensitivity ELISA Kit [cat. no. EK182HS; Hangzhou Multi Sciences (Lianke) Biotech Co., Ltd.], Human IL-8 ELISA Kit [cat. no. EK108; Hangzhou Multi Sciences (Lianke) Biotech Co., Ltd.], a human IL-1β ELISA kit [EH0185; Hangzhou Multi Sciences (Lianke) Biotech Co., Ltd.] and IL-6 [cat. no. EK1217; Hangzhou Multi Sciences (Lianke) Biotech Co., Ltd.] according to the manufacturer's instructions.

For the mouse experiments, all mice were anesthetized, and tracheal intubation was performed through the midline of the neck. A total of 30 mice (n=6 in each group) were used in the present study. The trachea was isolated, and the right main bronchus was ligated. Two milliliters of physiological saline were slowly injected into and then removed from the left lung using a syringe, and this procedure was repeated three times to collect bronchoalveolar lavage fluid (BALF). The BALF was centrifuged at 3,000 x g for 10 min at 4˚C, and the supernatant was collected. TNF-α, IFN-γ, and IL-6, IL-10 levels in the BALF were measured using Mouse Tumor necrosis factor α, TNF-α ELISA KIT (cat. no. CSB-E04741m; Cusabio Technology, LLC), Mouse Interferon γ, IFN-γ/interferon, gamma/Ifng ELISA Kit (cat. no. CSB-E04578m; Cusabio Technology, LLC) and Mouse IL-10 ELISA Kit (cat. no. U96-1517E; YOBIBIO (Shanghai) Biotechnology Co., Ltd.).

TP attenuates H1N1-triggered pneumonia pathogenesis in a co-culture model. In the present study, the primary aim was to investigate the therapeutic effect of TP on H1N1-induced pneumonia, with particular focus on the two key cell types that play critical roles in the development and progression of viral pneumonia: alveolar epithelial cells and immune cells. HBEpiC cells were used as an *in vitro* model of human bronchial/alveolar epithelial cells, which are the primary targets for H1N1 virus infection in the respiratory tract. Infection of these cells initiates viral replication and triggers local inflammatory responses, leading to epithelial damage and impaired lung function. THP-1 cells are a well-established human monocytic cell line commonly used to simulate monocytes/macrophages *in vitro*. These cells are representative of the innate immune cells recruited to the lungs during influenza infection, where they participate in the antiviral response and contribute to the release of pro-inflammatory cytokines, which can amplify lung inflammation and tissue injury. By using HBEpiC and THP-1 cells, the present study aimed to recreate an *in vitro* co-culture context that mimicked the interactions between infected epithelial cells and responding immune cells, thus allowing it to evaluate whether TP can modulate both virus-induced epithelial damage and the excessive immune-inflammatory response that underlies the pathogenesis of H1N1-induced pneumonia.

Adhesion assay between THP-1 cells and HBEpiCs. An adhesion assay was performed as an integral component of the investigation into the interactions between HBEpiCs and monocytes (THP-1) during H1N1 influenza virus infection. This assay aimed to simulate and quantify the recruitment and adhesion of immune cells to the alveolar epithelium, a critical step in the initiation and propagation of pulmonary inflammation during viral infections. THP-1 cells were induced with PMA for 24 h as previously described. Simultaneously, HBEpiCs were transfected with a GFP-tagged fluorescent adenovirus (30 MOI; Charles River Laboratories). After 24 h, the transfected HBEpiCs were collected. These GFP-labeled HBEpiCs were then added to the pretreated THP-1 cells and both cell types were cocultured for an additional 24 h. In the TP intervention group, TP at concentrations of 5, 10 and 20 nM (Beijing Solarbio Science & Technology Co., Ltd.) was added for another 24 h of culture. The adhesion between THP-1 cells and HBEpiCs was observed and evaluated under a fluorescence microscope (20x; Olympus Corporation).

Cell migration assay. A cell migration assay was used to investigate the chemotactic response of monocyte-derived THP-1 cells to soluble factors secreted by H1N1-infected HBEpiCs. This approach aimed to simulate the *in vivo* recruitment of immune cells to sites of viral infection, a critical component of the inflammatory response in H1N1-induced pneumonia. THP-1 cells were seeded into the upper chamber of a Transwell insert and induced with phorbol myristate acetate (PMA) for 24 h as aforementioned. HBEpiCs were infected with H1N1 virus, and the culture supernatant was collected after 24 h. The supernatant was then placed in the lower chamber of the

Transwell insert. After 24 h of incubation, the migration of THP-1 cells to the lower chamber was observed. Migrated cells were counted and quantified via microscopy. The number of cells that migrated through the membrane was used as an indicator of cell migration.

Reverse transcription-quantitative (RT-q) PCR

Viral RNA quantification (absolute quantification). Lung tissue stored at -80˚C was homogenized in liquid nitrogen to obtain a fine powder. RNA was extracted using Triquick Reagent (cat. no. R1100; Beijing Solarbio Science & Technology Co., Ltd.) and stored at -80˚C. DEPC-treated water (DEPC-H2O) was used as a negative control. For absolute quantification of the viral load, a standard curve was generated using positive controls prepared by serially diluting a standard sample with a known concentration to final concentrations of $1x10^7$, $1x10^6$, $1x10^5$, $1x10^4$ and $1x10^3$ copies/ml. For each reaction using the H1N1 Subtype Influenza A (Avian Influenza) Dual RT-PCR Detection Kit (cat. no. LM82068SRP; Shanghai Lianmai Biological Engineering Co., Ltd.) 18 μl of master mix, 1 μl of internal control and 1 μl of RT-PCR enzyme mixture were added. The mixture was vortexed and centrifuged briefly at 3,000 x g. A total of 20 μl of the resulting mixture was transferred to a PCR tube, followed by the addition of 5 μl of sample nucleic acid extract, DEPC-H_2O (negative control), or diluted positive control (standard curve points). The samples were then centrifuged and immediately subjected to PCR amplification: Reverse transcription: 50˚C for 15 min; initial denaturation: 95˚C for 5 min; cycling program (number of cycles: 40): Denaturation: 95˚C for 15 sec; annealing/extension: 58˚C for 60 sec). The cycle threshold (Cq) values obtained for the samples and the standard curve points were recorded. The viral nucleic acid concentration (copies/ml) in each sample was determined by interpolating its Cq value onto the standard curve ($\log_{10}$ copies/ml vs. Cq value) generated from the diluted positive controls (23).

Cellular gene expression analysis (relative quantification). In addition, total RNA was collected and extracted from the cell samples. First-strand cDNA synthesis was performed using the Invitrogen; Thermo Fisher Scientific, Inc. SuperScript IV UniPrime Kit (Invitrogen; Thermo Fisher Scientific, Inc.) according to the manufacturer's instructions. Subsequently, quantitative real-time PCR was performed using NovoStart® SYBR High-Sensitivity qPCR SuperMix (Novoprotein Scientific Inc.). Relative gene expression levels were determined via the comparative Cq ($\Delta\Delta$Cq) method (23). The expression of the target gene(s) was normalized to that of GAPDH. The sequences of primers used in the present study: AIM2-F: TAGCGCCTCACGTGTGTTAG, AIM2-R: TCG GGGTTTCACCAGCTTTT; Caspase-1-F: GGGAGTGTG GGAAGGTTGAG, Caspase-1-R: GTGCTCTGCACTGAC CAGAA; GSDMD-F: CCTCTCCATGATGAGGTGCC, GSDMD-R: CCCAGCAGGTAGACAACAGG; GAPDH-F: CCAGCAAGAGCACAAGAGGA, GAPDH-R: GGGGAG ATTCAGTGTGGTGG.

Western blot analysis. The proteins were extracted using RIPA buffer (high; Beijing Solarbio Science & Technology Co., Ltd., Beijing, China) supplemented with 1 mM PMSF (Beijing Solarbio Science & Technology Co., Ltd.) and 1X protease inhibitor cocktail (cat. no. A8260; Beijing Solarbio Science & Technology Co., Ltd.). Cell or tissue lysates were collected and centrifuged at 15,000 x g for 10 min at 4˚C. Protein concentrations were determined via a BCA assay kit. Proteins (10 μg/lane) were separated by 12% SDS-PAGE and transferred onto a PVDF membrane at 4˚C. The membrane was blocked with 5% bovine serum albumin at room temperature for 1 h, followed by overnight incubation with primary antibodies targeting AIM2 (cat. no. TB7010S), caspase-1 (cat. no. TA5418S), GSDMD (cat. no. TA4012S) and β-actin (cat. no. P30002; 1:1,000; all from Abmart Pharmaceutical Technology Co., Ltd.). The membrane was then incubated with ActivAb Goat Anti-Rabbit IgG/HRP secondary antibody (1:5,000, cat. no. SE134, Beijing Solarbio Science & Technology Co., Ltd.) at 37˚C for 2 h. Protein bands were visualized using an enhanced chemiluminescence reagent (Beijing Solarbio Science & Technology Co., Ltd.), and the signal intensities of the target bands were quantified using ImageJ software (version number: 1.8.0, National Institutes of Health).

Dual-immunofluorescence staining. To investigate the assembly of the AIM2 inflammasome during viral infection, the present study performed dual-immunofluorescence staining for ASC (an adaptor protein) and AIM2 (a cytosolic DNA sensor). The colocalization of these two proteins (visualized as overlapping fluorescent signals) indicates the formation of the ASC-AIM2 inflammasome complex, a key event in innate immune activation. THP-1 cells and HBEpiCs were seeded at a density of $1x10^5$ cells/ml onto glass slides and cultured in a 6-well plate for 24 h. The cells were fixed at room temperature using 4% paraformaldehyde (PFA; Beijing Solarbio Science & Technology Co., Ltd.) in PBS for 10 min, followed by three 5-min washes with PBS. Blocking was performed at room temperature for 1 h. Blocking was performed using QuickBlock Blocking Buffer for Immunol Staining (P0260; Beyotime Institute of Biotechnology) at room temperature for 15 min. Primary antibodies targeting ASC and AIM2 were added, and the samples were incubated overnight at 4˚C. Then, fluorescently labeled anti-rabbit or anti-mouse secondary antibodies (Beijing Solarbio Science & Technology Co., Ltd.) were applied and incubated with the samples at room temperature for 1 h. Following secondary antibody incubation and washing, the cells were stained with DAPI (1 μg/ml in PBS) for 5 min at room temperature to visualize cell nuclei. The cells were washed three times with PBS for 5 min each. Finally, anti-fade mounting medium (Beijing Solarbio Science & Technology Co., Ltd.) was applied to the slides, and the cells were observed under a fluorescence microscope at a magnification of x20.

LDH release cytotoxicity assay. Cells in both experimental and control groups were seeded into 96-well plates at 100 μl per well and allowed to grow until reaching approximately 70-80% confluency before treatment. The following controls were included: A blank control (medium only, no cells), a spontaneous release control (untreated cells), and a maximum release control (cells fully lysed by addition of lysis buffer as per manufacturer's instructions). After treatment, 50 μl of the supernatant from each well was transferred to a new

plate, and an equal volume of LDH reaction mix from the Lactate Dehydrogenase (LDH) Activity Assay Kit (cat. no. E-BC-K046-M; Elabscience Bionovation Inc.) was added. The reaction was incubated at room temperature in the dark for 20 min, then stopped with stop solution. Absorbance was measured at 450 nm using a microplate reader. Background absorbance (blank) was subtracted from all sample values to yield corrected OD readings.

Ad-AIM2 transfection. To confirm AIM2 as a key functional target through which TP exerts its immunosuppressive effects, a rescue experiment was performed in which AIM2 was overexpressed in THP-1-derived macrophages. Ad-AIM2 was constructed by Hanheng Biotechnology (Shanghai) Co., Ltd. After 24 h of PMA induction in THP-1 cells, the cells were transfected with a viral vector containing Ad-AIM2 at 30 MOI for 24 h. Following transfection, subsequent experiments were conducted as aforementioned.

In vivo mouse model of H1N1 influenza virus infection and TP treatment. To evaluate the therapeutic efficacy of TP against influenza virus infection *in vivo*, a murine model of H1N1 influenza virus-induced pneumonia was established. Specific pathogen-free (SPF)-grade male C57BL/6 mice (8 weeks old; weighing 20-22 g; n=30) were purchased from Cyagen Biosciences (Guangzhou) Co., Ltd. The mice were housed in an SPF barrier facility at Guangzhou University of Chinese Medicine under controlled environmental conditions consisting of a temperature of 22±2˚C, a humidity of 55±10%, and a 12-h light/dark cycle (lights on at 7:00 am). The animals were provided standard laboratory rodent chow and autoclaved water *ad libitum*. The mice were acclimatized to the housing conditions for at least 7 days prior to any experimental procedures. All experimental procedures were performed in accordance with the guidelines of the Institutional Animal Care and Use Committee and approved by the Committee on the Ethics of Animal Experiments of Guangzhou University of Chinese Medicine (approval no. 2024055R).

Virus and infection. The influenza A virus strain A/Puerto Rico/8/1934 (H1N1; PR8) was obtained from the American Type Culture Collection. The virus was propagated in Madin-Darby canine kidney (MDCK) cells and purified. The viral titer was determined by plaque assay. For infection, the mice were lightly anesthetized via inhalation of isoflurane (4% induction, 2% maintenance) and intranasally inoculated with 100 μl of a viral suspension containing $1x10^5$ plaque-forming units (PFUs) of PR8 virus (diluted in sterile saline to a concentration of $1x10^6$ PFU/ml). For model establishment, control mice were inoculated intranasally with an equivalent volume (100 μl) of sterile saline under identical anesthesia conditions.

Model confirmation. At 6 days post-infection, all mice in the virus-infected group (n=5) and saline control group (n=5) were sacrificed by cervical dislocation under deep anesthesia (5% isoflurane inhalation, with the absence of the pedal reflex confirmed). Lung tissues were collected for histopathological analysis by hematoxylin and eosin (H&E) staining. Successful model establishment was defined as >90% of infected mice exhibiting characteristic viral pneumonia features (inflammatory cell infiltration, hemorrhage, atelectasis, interstitial edema, and alveolar wall thickening), with control mice showing no significant pathology.

Group assignment and treatment. Following confirmation of successful model establishment, H1N1-infected mice were randomly divided into five experimental groups (n=5 per group): i) H1N1 control (model control): infected, treated with vehicle (sterile saline via oral gavage); ii) Tamiflu: infected, treated with Tamiflu (oseltamivir phosphate, 20 mg/kg via oral gavage; this dose was selected on the basis of its well-established efficacy in murine models of H1N1 infection, as reported in previous studies (24,25), and aligns with doses commonly used to demonstrate significant antiviral activity and survival benefit in this context); iii) L-TP: infected, treated with low-dose TP (5 $\mu g \cdot kg^{-1} \cdot day^{-1}$ via intraperitoneal injection); iv) M-TP: infected, treated with medium-dose TP (10 $\mu g \cdot kg^{-1} \cdot day^{-1}$ via intraperitoneal injection); and v) H-TP: infected, treated with high-dose TP (20 $\mu g \cdot kg^{-1} \cdot day^{-1}$ via intraperitoneal injection) (26). vi) Additionally, the initial saline control (uninfected control) group (n=5) was maintained as an uninfected, untreated control. Treatments commenced at 48 h post-infection and were administered twice daily (morning and afternoon) by oral gavage for 5 consecutive days. The gavage volume for all treatments was standardized at 0.2 ml per 10 g of body weight. Animals in the uninfected control group and H1N1 control group received equivalent volumes of sterile saline via oral gavage.

Terminal procedures and sample collection. At the end of the treatment period (day 7), all mice were weighed and sacrificed. Prior to sacrifice, mice were deeply anesthetized with isoflurane (4% induction, 2% maintenance). Following sufficient anesthesia, sacrifice was performed by cervical dislocation or another approved method in accordance with ethical guidelines. The lungs were aseptically removed. The left lung lobe was fixed in 4% PFA at room temperature for 15 min subsequent histopathological analysis. The right lung lobes were snap-frozen in liquid nitrogen and stored at -80˚C for further biochemical/molecular analyses. For immediate analysis, a portion of frozen lung tissue from the right lung was homogenized in 1 ml of ice-cold sterile saline using a tissue homogenizer. The homogenate was centrifuged at 3,000 x g and 4˚C for 10 min, and the supernatant was collected and stored at -80˚C until analysis.

Assessment parameters. The lung index was calculated as follows: (lung wet weight/body weight) x100%. The lung index inhibition rate for the treatment groups was calculated using the following formula: lung index inhibition rate (%)=[(mean lung index_H1N1 control-mean lung index_treatment group)/(mean lung index_H1N1 control-mean lung index_uninfected control)] x100%.

H&E staining. A total of 30 mice from each group (n=5 in each group) were sacrificed, and their lungs were dissected. The left lung was fixed in 4% paraformaldehyde (Beijing Solarbio Science & Technology Co., Ltd.), dehydrated in a graded ethanol series and embedded in paraffin. Sections with a thickness of 4 μm were prepared. H&E staining was

performed at room temperature (~25˚C), as per the standard protocol provided with the kit (Beijing Solarbio Science & Technology Co., Ltd.). The pathological changes in the lung tissue were then observed under a light microscope. Two well-established semiquantitative histopathological scoring systems were used to assess lung injury in our study. Specifically, the first was reported by Zeldin *et al* (27): This method is used to evaluate lung injury based on parameters such as perivascular edema, inflammatory cell infiltration, and alveolar damage. Each parameter is scored on a scale from 0 to 4, with higher scores indicating more severe injury. The second was reported by Matute-Bello *et al* (28) and is recommended by the American Thoracic Society: This system assesses five key histological features, including alveolar and interstitial neutrophil infiltration, hyaline membrane formation, proteinaceous debris in airspaces, and alveolar septal thickening. Each feature is scored from 0 to 2 across multiple high-power fields, and the total score provides a quantitative measure of lung injury severity.

Statistical analysis. All experiments were independently repeated three times. Statistical analysis of the experimental data was performed via GraphPad Prism 8.0 software. Data that followed a normal distribution are presented as the mean ± standard deviation. Intergroup comparisons were performed using one-way ANOVA, followed by Tukey's post hoc test. $P<0.05$ was considered to indicate a statistically significant difference.

Results

H1N1 infection induces cytotoxicity and modulates inflammatory responses in HBEpiCs and THP-1 cells. The present study infected HBEpiCs with H1N1 and observed a concentration-dependent decrease in cell viability following infection (Fig. 1A). Moreover, the levels of the inflammatory cytokines IL-1β, IL-6, TNF-α, and IL-8 in HBEpiCs increased following H1N1 infection (Fig. 1B). Furthermore, the supernatant from H1N1-infected HBEpiCs was collected and added to THP-1 cell cultures. The results revealed a gradual reduction in THP-1 cell viability in response to increasing H1N1 concentration (Fig. 1C). Similarly, the levels of IL-1β, IL-6, TNF-α, and IL-8 in THP-1 cells also increased following H1N1 infection (Fig. 1D). Additionally, the adhesion between THP-1 cells and HBEpiCs was assessed and it was observed that the number of THP-1 cells adhering to HBEpiCs increased with increasing H1N1 concentration (Fig. 1E). Moreover, the migration capacity of THP-1 cells increased as the H1N1 concentration increased (Fig. 1F). These findings suggested a potential interaction between these cells under inflammatory conditions induced by the virus.

H1N1 infection activates AIM2 signaling in THP-1 cells but not in HBEpiCs. AIM2 regulation plays a crucial role in the pathogenesis of H1N1-induced lung diseases, serving as an important component of the antiviral response while potentially exacerbating pathological damage (29). Therefore, the present study focused on investigating whether H1N1 infection alters the AIM2 signaling pathway in alveolar epithelial cells and immune cells. The RT-qPCR results revealed that H1N1 infection did not affect AIM2 mRNA levels in HBEpiCs but markedly increased AIM2 mRNA levels in THP-1 cells (Fig. 2A). Additionally, lactate dehydrogenase (LDH) release was assessed and found that H1N1 infection did not affect the LDH release rate in HBEpiCs but markedly increased the release of LDH-1 in THP-1 cells (Fig. 2B). Furthermore, dual-immunofluorescence staining revealed the formation of a complex between ASC and AIM2 in THP-1 cells (Fig. 2C). Compared with the control, H1N1 infection did not markedly alter the protein levels of AIM2, caspase-1, or GSDMD in HBEpiCs (Fig. 2D). However, in THP-1 cells, H1N1 infection led to increased protein levels of AIM2, caspase-1, and GSDMD (Fig. 2E). Following infection of HBEpiCs with H1N1 virus at an MOI of 5 for 24 h, no significant cell death was observed among HBEpiCs (Fig. 2F). The supernatants from both the control and H1N1-infected HBEpiC groups were subsequently collected and used to treat THP-1 cells for an additional 24 h. Compared with that in the control (Con) group, the death rate in the treated THP-1 cell group was markedly greater (Fig. 2G). Overall, H1N1 infection activated the AIM2 signaling pathway and increased cell death among THP-1 cells, whereas it did not activate the AIM2 signaling pathway or induce cell death among HBEpiCs. These results highlighted the differential responses of different cell types to H1N1 infection. Immune cells exert their effects through AIM2-mediated inflammatory responses, whereas epithelial cells may use other mechanisms for antiviral defense. However, the factors they release can still influence immune cell behavior, further exacerbating the immune response and cell death.

TP inhibits the inflammatory response and immune cell activity in H1N1-Infected HBEpiCs and THP-1 cells. The concentration gradient of TP (5, 10, 20, 30 nM) was designed based on established literature evidence and fundamental biological differences between cell models. Zhou *et al* (29) demonstrated that 10 nM TP markedly reduces viability in immortalized human bronchial epithelial cells (BEAS-2B) within 24 h in an acute lung injury model. Additionally, *in vitro* experiments with primary mouse lung fibroblasts showed that TP concentrations ranging from 10-40 nM gradually inhibited cell viability, with concentrations >40 nM exhibiting marked cytotoxicity (30). Therefore, 20 and 40 nM were selected or subsequent experiments to balance efficacy and cytotoxicity. Consequently, 5, 10, 20 and 30 nM were selected for the preliminary dose-response experiments to evaluate antiviral efficacy while minimizing cytotoxic effects. Cell viability assays indicated that 5, 10, and 20 nM TP did not markedly affect HBEpiC viability compared with the control, whereas 30 nM TP led to a noticeable decrease in cell viability (Fig. 3A). Based on these findings, 5, 10, and 20 nM TP were selected for subsequent experiments for assessing antiviral efficacy. However, following TP treatment, the levels of IL-1β, IL-6, TNF-α, and IL-8 in HBEpiCs were markedly reduced (Fig. 3B). By contrast, when TP was applied to THP-1 cells pretreated with the supernatant from H1N1-infected HBEpiC cultures, the viability of the THP-1 cells decreased (Fig. 3C). Additionally, the levels of IL-1β, IL-6, TNF-α, and IL-8 in THP-1 cells were markedly lower after TP treatment (Fig. 3D). Moreover, the adhesion of THP-1 cells to HBEpiCs induced by

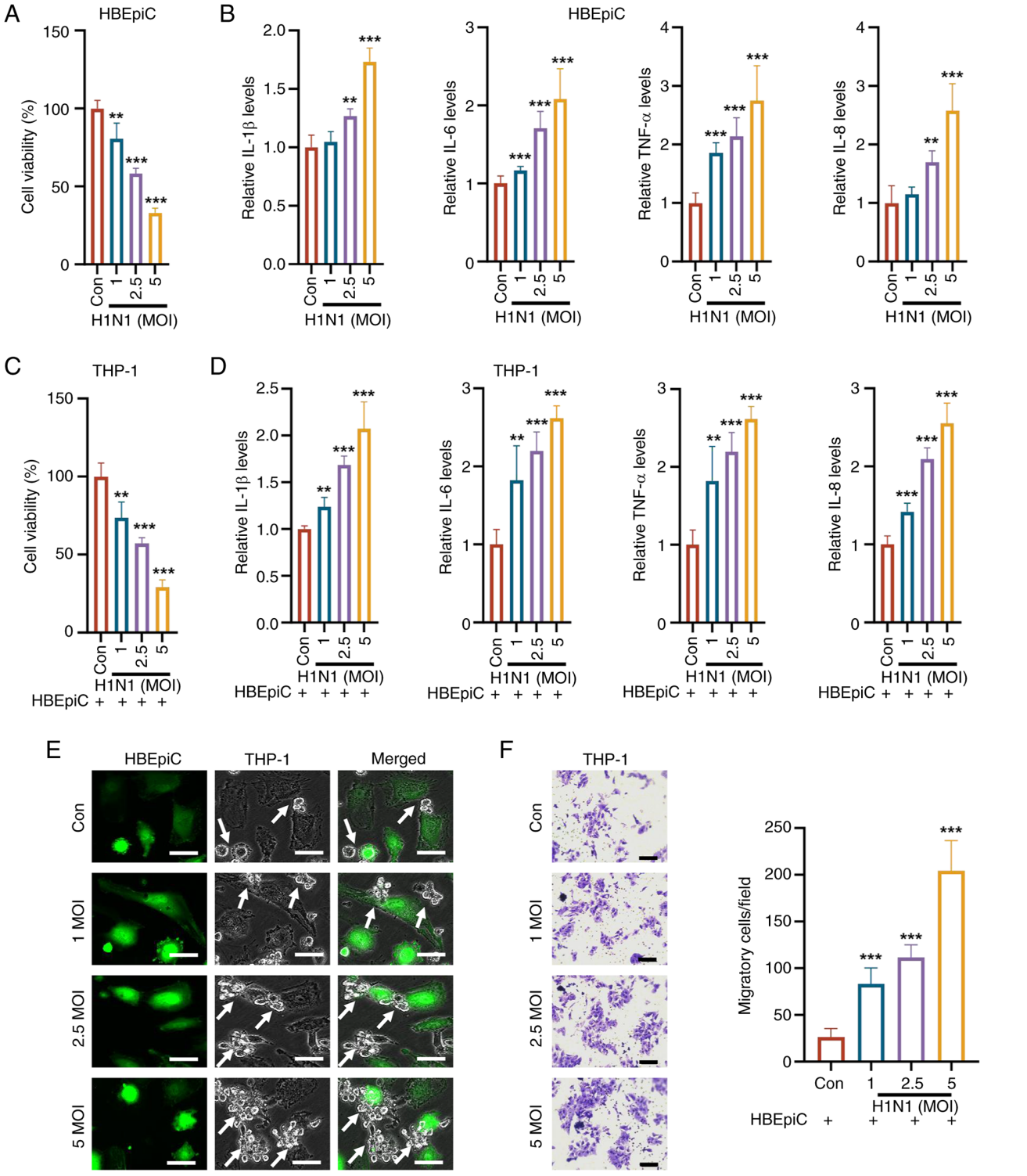

Figure 1. H1N1 infection affects cell viability, inflammatory cytokine secretion and interactions between HBEpiCs and THP-1 cells. (A) CCK-8 assay revealed that HBEpiC viability decreased in a concentration-dependent manner following H1N1 infection. (B) ELISA revealed that the levels of IL-1β, IL-6, TNF-α, and IL-8 in HBEpiCs decreased with increasing H1N1 infection. (C) CCK-8 assay indicated that supernatants from H1N1-infected HBEpiC cultures reduced the viability of THP-1 cells in a dose-dependent manner. (D) ELISA results suggested that the levels of inflammatory cytokines (IL-1β, IL-6, TNF-α and IL-8) in THP-1 cells were decreased following exposure to supernatants from H1N1-infected HBEpiC cultures. (E) Cell adhesion assay revealed that the number of THP-1 cells adhering to HBEpiCs increased with increasing H1N1 concentration (scale bar, 10 μm). Arrow indicates THP-1 cells that remain attached to the surface of HBEpiCs, highlighting the adhesion interaction between the two cell types. (F) Transwell assay suggested that H1N1 infection enhanced the migration capacity of THP-1 cells, with increased migration observed at higher virus concentrations (scale bar, 50 μm). The data are presented as the mean ± standard deviation; **P<0.01, ***P<0.001 vs. control. H1N1, influenza A; HBEpiCs, human bronchial epithelial cells; ELISA, enzyme-linked immunosorbent assay; IL, interleukin; TNF-α, tumor necrosis factor-α; Con, control; MOI, multiplicity of infection.

H1N1 infection was reduced in a dose-dependent manner with increasing TP concentrations (Fig. 3E). Similarly, when the supernatant collected from H1N1-infected HBEpiC cultures were treated with TP, the migration capacity of the THP-1 cells

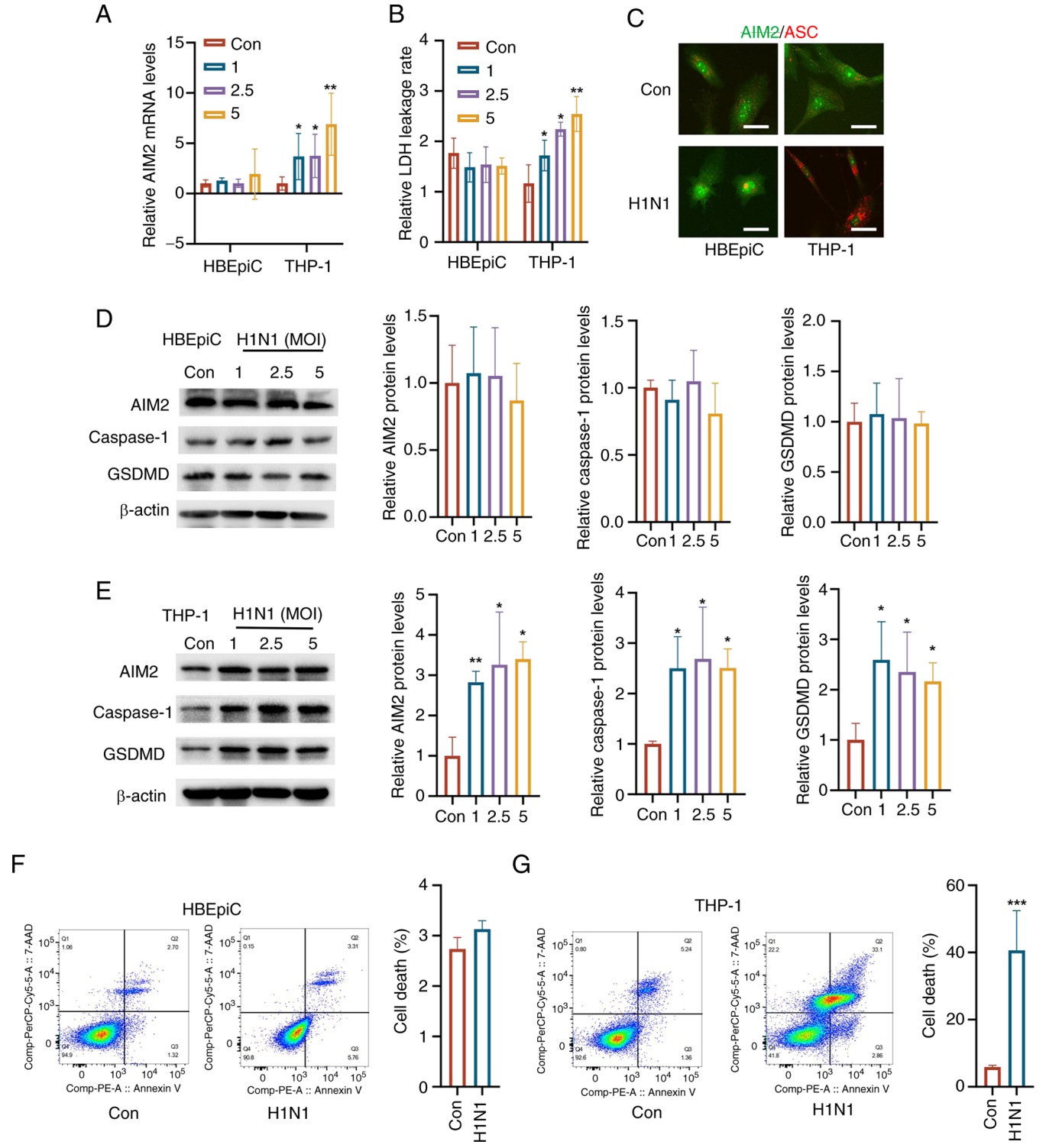

Figure 2. Differential activation of AIM2 signaling in THP-1 cells and HBEpiCs following H1N1 infection. (A) RT-qPCR analysis revealed that H1N1 infection did not alter AIM2 mRNA levels in HBEpiCs but markedly increased AIM2 mRNA levels in THP-1 cells. (B) LDH release assay indicated that H1N1 infection did not affect LDH release in HBEpiCs but markedly increased LDH-1 release in THP-1 cells. (C) Dual-immunofluorescence staining demonstrated the formation of ASC-AIM2 complexes in THP-1 cells post-H1N1 infection (scale bar, 10 μm). (D) Western blot analysis revealed no significant changes in AIM2, caspase-1, or GSDMD protein levels in HBEpiCs following H1N1 infection but increased expression of AIM2, caspase-1 and GSDMD in THP-1 cells following H1N1 infection (E). (F) Flow cytometry analysis revealed no significant cell death in HBEpiCs following infection, (G) whereas THP-1 cells treated with the supernatant from H1N1-infected HBEpiC cultures presented markedly increased cell death compared with the control. The data are presented as the mean ± standard deviation; *P<0.05, **P<0.01, ***P<0.001 vs. control. AIM2, absent in melanoma 2; HBEpiCs, human bronchial epithelial cells; H1N1, influenza A; RT-qPCR, reverse transcription-quantitative PCR; GSDMD, gasdermin D; Con, control; MOI, multiplicity of infection.

was also markedly reduced (Fig. 3F). These findings suggested that TP, as an immunomodulator, may regulate the inflammatory response by inhibiting the overactivation of immune cells.

TP suppresses AIM2 signaling, induces pyroptosis in THP-1 cells, and alleviates inflammatory damage to HBEpiCs. Following H1N1 infection of HBEpiCs, TP was administered

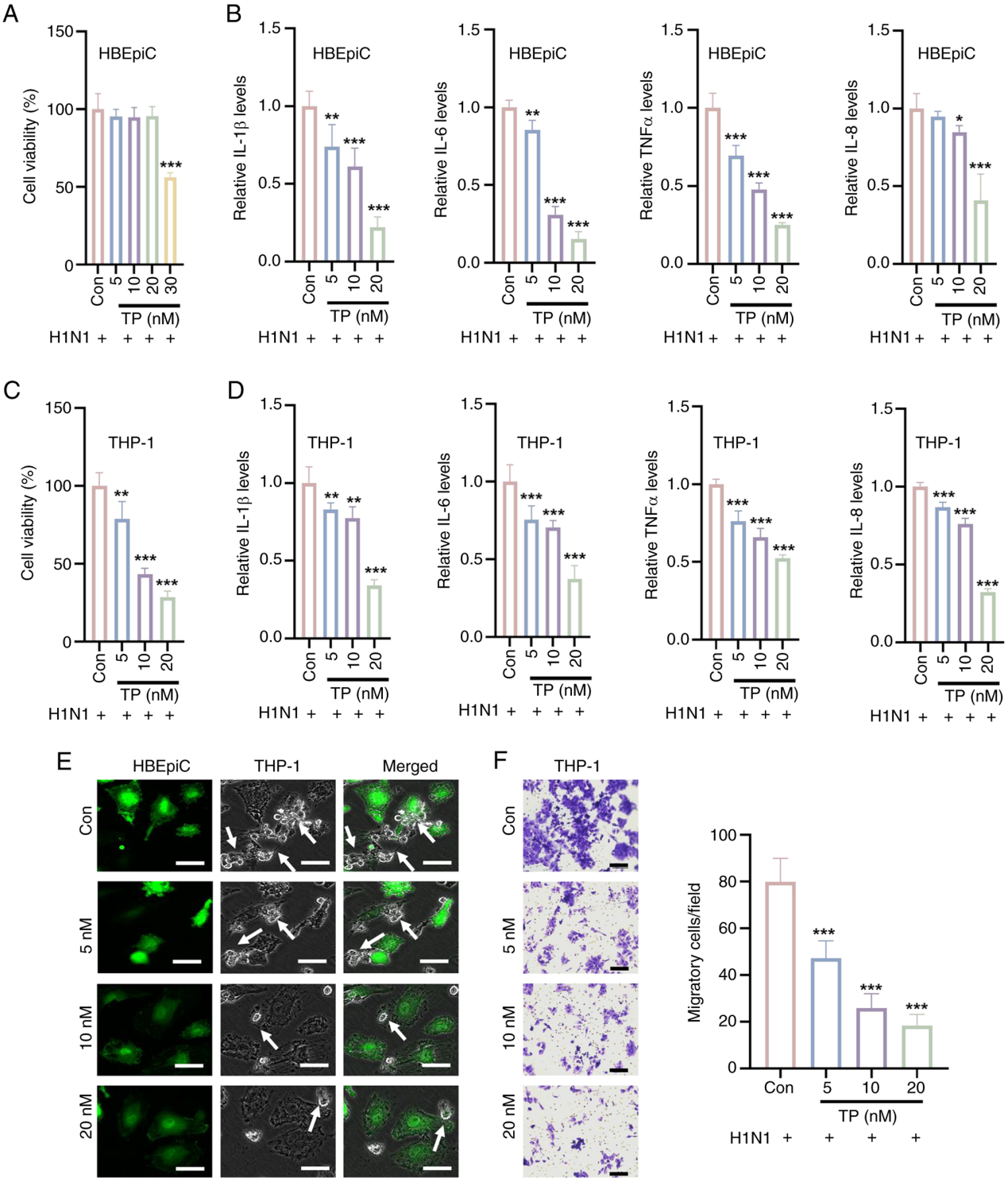

Figure 3. TP modulates the inflammatory response and immune cell activity in H1N1-infected HBEpiCs and THP-1 cells. (A) No significant changes were observed in HBEpiCs treated with various concentrations of TP (5, 10 and 20 nM) following H1N1 infection compared with the control. (B) After TP treatment, the levels of the inflammatory cytokines IL-1β, IL-6, TNF-α and IL-8 in HBEpiCs were markedly lower than those in the untreated group. (C) The viability of THP-1 cells pretreated with H1N1-infected HBEpiC culture supernatant decreased after TP treatment. (D) The levels of IL-1β, IL-6, TNF-α, and IL-8 in THP-1 cells were markedly lower after TP treatment. (E) The adhesion of THP-1 cells to HBEpiCs induced by H1N1 infection decreased in a dose-dependent manner with increasing TP concentration (scale bar, 10 μm). Arrow indicates THP-1 cells that remain attached to the surface of HBEpiCs, highlighting the adhesion interaction between the two cell types. (F) The migration capacity of THP-1 cells was markedly reduced when the supernatant from H1N1-infected HBEpiC cultures was treated with TP (scale bar, 50 μm). The data are presented as the mean ± standard deviation; *P<0.05, **P<0.01, ***P<0.001 vs. control. TP, triptolide; H1N1, influenza A; HBEpiCs, human bronchial epithelial cells; IL, interleukin; TNF-α, tumor necrosis factor-α; Con, control.

and the culture supernatant was collected to pretreat THP-1 cells. In HBEpiCs, TP treatment did not affect the mRNA level of AIM2, whereas in THP-1 cells, the mRNA expression of AIM2 was markedly reduced by TP treatment (Fig. 4A). Additionally, TP treatment of HBEpiCs did not alter the LDH leakage rate, but in THP-1 cells, TP reduced the LDH leakage

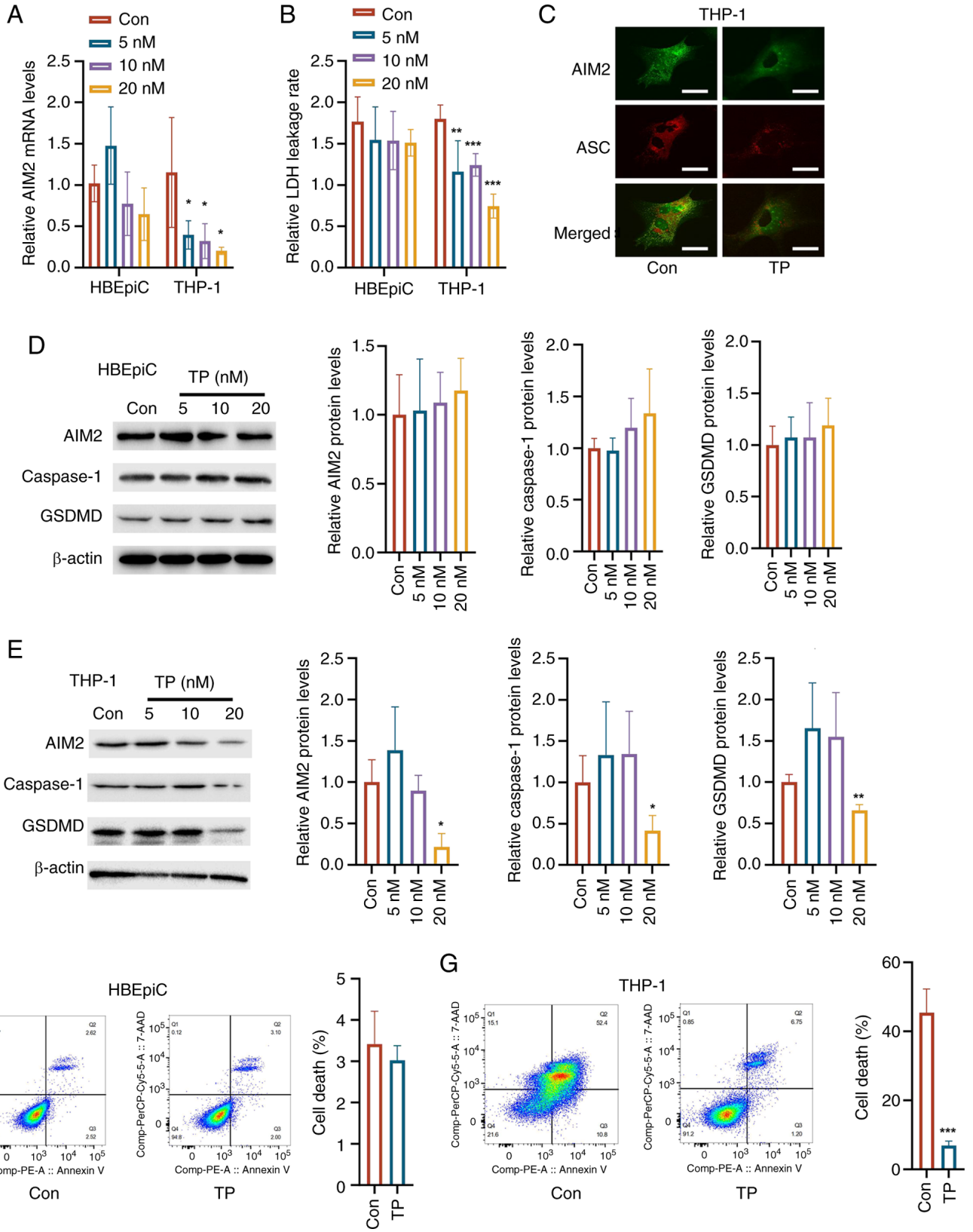

Figure 4. Effects of TP on AIM2 signaling, LDH leakage, and pyroptosis in HBEpiCs and THP-1 cells. (A) RT-qPCR analysis revealed that TP treatment did not alter AIM2 mRNA expression in HBEpiCs but markedly reduced AIM2 mRNA levels in THP-1 cells. (B) TP did not affect the LDH leakage rate in HBEpiCs but markedly reduced LDH leakage in THP-1 cells. (C) Dual-fluorescence staining revealed that TP treatment decreased the formation of ASC-AIM2 complexes in THP-1 cells (scale bar, 10 μm). (D) Western blot analysis indicated that TP treatment did not markedly affect the expression of these proteins in HBEpiCs. (E) TP treatment reduced the protein expression of AIM2, caspase-1, and GSDMD in THP-1 cells. (F) Flow cytometry revealed no difference in cell death between HBEpiCs treated with 20 nM TP and the control. (G) In THP-1 cells infected with H1N1 and treated with 20 nM TP, a significant reduction in cell death was identified compared with that in the H1N1 infection group. The data are presented as the mean ± standard deviation; *P<0.05, **P<0.01, ***P<0.001 vs. control. TP, triptolide; AIM2, absent in melanoma 2; LDH, lactate dehydrogenase; HBEpiCs, human bronchial epithelial cells; RT-qPCR, reverse transcription-quantitative PCR; H1N1, influenza A; GSDMD, gasdermin D; Con, control.

rate (Fig. 4B). Furthermore, dual-fluorescence staining of THP-1 cells revealed a decrease in the formation of ASC and AIM2 complexes (Fig. 4C). In HBEpiCs, TP treatment did not markedly affect the protein expression of AIM2, caspase-1, or GSDMD (Fig. 4D). However, in THP-1 cells, TP treatment decreased the protein expression of AIM2, caspase-1, and GSDMD (Fig. 4E). Additionally, at 20 nM, TP did not affect the death rate of HBEpiCs but markedly mitigated the increased death rate of THP-1 cells induced by H1N1 infection (Fig. 4F and G). These results indicated that TP exerted differential effects on different cell types and that its anti-inflammatory action is mediated primarily by the inhibition of AIM2-mediated cell death and inflammatory responses.

AIM2 overexpression reverses the immunosuppressive effects of TP in THP-1 cells. To confirm that AIM2 is a key target of TP in THP-1 cells, AIM2 was overexpressed in THP-1 cells. The data showed that transfection with Ad-AIM2 markedly upregulated the expression of AIM2 in THP-1 cells compared with that of Ad-NC (Fig. 5A). HBEpiCs were incubated with H1N1 and the supernatant was collected to treat AIM2-overexpressing THP-1 cells with or without TP treatment. Compared with those in THP-1 cells without AIM2 overexpression, AIM2 protein levels were elevated in AIM2-overexpressing THP-1 cells (Fig. 5B). In THP-1 cells, after TP treatment, the LDH leakage rate was lower than that in the control group of cells treated with H1N1 alone. However, overexpression of AIM2 increased the LDH leakage rate (Fig. 5C). Moreover, AIM2 overexpression reversed the reduction in adhesion between THP-1 cells and HBEpiCs induced by TP treatment (Fig. 5D). Furthermore, AIM2 overexpression enhanced the migration ability of THP-1 cells compared with that of control cells treated with H1N1 alone (Fig. 5E). Notably, AIM2 overexpression even reversed the decrease in THP-1 cell migration induced by TP treatment (Fig. 5E). Additionally, AIM2 overexpression reversed the reduction in the levels of various inflammatory cytokines caused by TP treatment in THP-1 cells (Fig. 5F). These findings suggested that TP exerts its immunosuppressive effects by modulating AIM2 signaling, thereby preventing overactivation of immune cells and reducing inflammation.

TP alleviates lung injury in a murine H1N1 pneumonia model. To further investigate the effect of TP *in vivo*, a murine pneumonia model induced by H1N1 infection was established. Histological analysis with H&E staining revealed that, compared with that of model mice, the lung tissue of normal mice presented a clear structure with no thickening of the alveolar septa, no infiltration of inflammatory cells in the stroma, and no abnormal changes in bronchial structure. By contrast, mice in the model group showed varying degrees of alveolar septal thickening and even consolidation of lung tissue. Compared with those in the model group, mice in the H-TP and Tamiflu treatment groups exhibited mild thickening of the alveolar septa, with markedly fewer histopathological changes. Additionally, compared with those in the model group, mice in the M-TP and L-TP groups presented varying degrees of improvement in the lung parenchyma, interstitial tissue and bronchial lesions (Fig. 6A). Furthermore, compared with those in the control group (0.1412±0.0035 g; 20.56±1.54 g), mice in the H1N1 treatment group presented increased lung weight and decreased body weight (0.1808±0.0022 g; 17.70±1.65 g) (Fig. 6B and C). The lung weight was markedly lower in the Tamiflu, M-TP and H-TP groups (0.1724±0.0030 g; 0.1700±0.0027 g; 0.1676±0.0122 g) than in the H1N1 group (0.1808±0.0022 g; Fig. 6B). However, there were no significant differences in body weight among the four treatment groups (18.84±1.81 g; 17.62±1.02 g; 18.52±1.50 g; 19.42±2.93 g) compared with the H1N1 group (17.70±1.65 g; Fig. 6C). The present study also analyzed the lung index, which was elevated following H1N1 infection (0.01029±0.00089) compared with that in the control group (0.00690±0.00050). After treatment in the four groups, the lung index did not fully recover (Tamiflu: 0.00922±0.00093; L-TP: 0.01044±0.00063; M-TP: 0.00922±0.00059; and H-TP: 0.00879±0.00140; Fig. 6D). Notably, the lung viral load was markedly lower in the Tamiflu (1.95±0.50), L-TP (4.90±0.45), M-TP (4.61±0.47), and H-TP (3.76±0.47) treatment groups compared with the H1N1 group (7.34±0.16), with the Tamiflu group showing the most prominent reduction (Fig. 6E). Additionally, the levels of inflammatory cytokines in the lung tissue were elevated following H1N1 infection (IL-6: 331.4±114.1 pg/ml; IL-10: 200.8±2.4 pg/ml; TNF-α: 82.0±15.2 pg/ml; IFN-γ: 169.4±3.2 pg/ml) compared with those in the control group (IL-6: 5.2±14.3 pg/ml; IL-10: 2.2±0.8 pg/ml; TNF-α: 3.6±1.8 pg/ml; IFN-γ: 8.2±1.3 pg/ml), but treatment with Tamiflu (IL-6: 106.8±25.2 pg/ml; IL-10: 39.6±12.3 pg/ml; TNF-α: 46.8±1.9 pg/ml; IFN-γ: 77.8±27.7 pg/ml), L-TP (IL-6: 199.0±47.3 pg/ml; IL-10: 95.8±13.1 pg/ml; TNF-α: 40.8±12.6 pg/ml; IFN-γ: 82.8±29.8 pg/ml), M-TP (IL-6: 128.4±50.2 pg/ml; IL-10: 55.4±13.9 pg/ml; TNF-α: 32.4±15.2 pg/ml; IFN-γ: 73.8±23.4 pg/ml), and H-TP (IL-6: 91.0±18.8 pg/ml; IL-10: 32.8±16.2 pg/ml; TNF-α: 32.6±8.8 pg/ml; IFN-γ: 45.6±18.6 pg/ml) markedly reduced these levels (Fig. 6F-I). Overall, TP demonstrated immune modulation at different doses, alleviating lung damage induced by H1N1 and reducing immune injury by regulating inflammatory responses and viral replication.

Discussion

Limitations of current Tamiflu therapy. Tamiflu is a commonly used antiviral medication for treating influenza A (H1N1), which works by inhibiting viral neuraminidase to slow viral replication, helping to alleviate symptoms and shorten the course of the disease (31). However, Tamiflu has several limitations. Its therapeutic efficacy is optimal within 48 h of symptom onset (31). Missing this window may result in reduced effectiveness. Some H1N1 strains may develop resistance, especially in immunocompromised patients (31). Additionally, Tamiflu primarily helps with symptom relief (32). It has limited efficacy in patients who have developed severe complications, such as acute respiratory distress syndrome (ARDS) or severe pneumonia (32). Tamiflu may also cause side effects, such as nausea and vomiting (32,33). Therefore, relying solely on Tamiflu may not fully address the complex pathology of H1N1 pneumonia. TP, an immunomodulatory agent, exerts multiple effects, including anti-inflammatory, immunosuppressive and

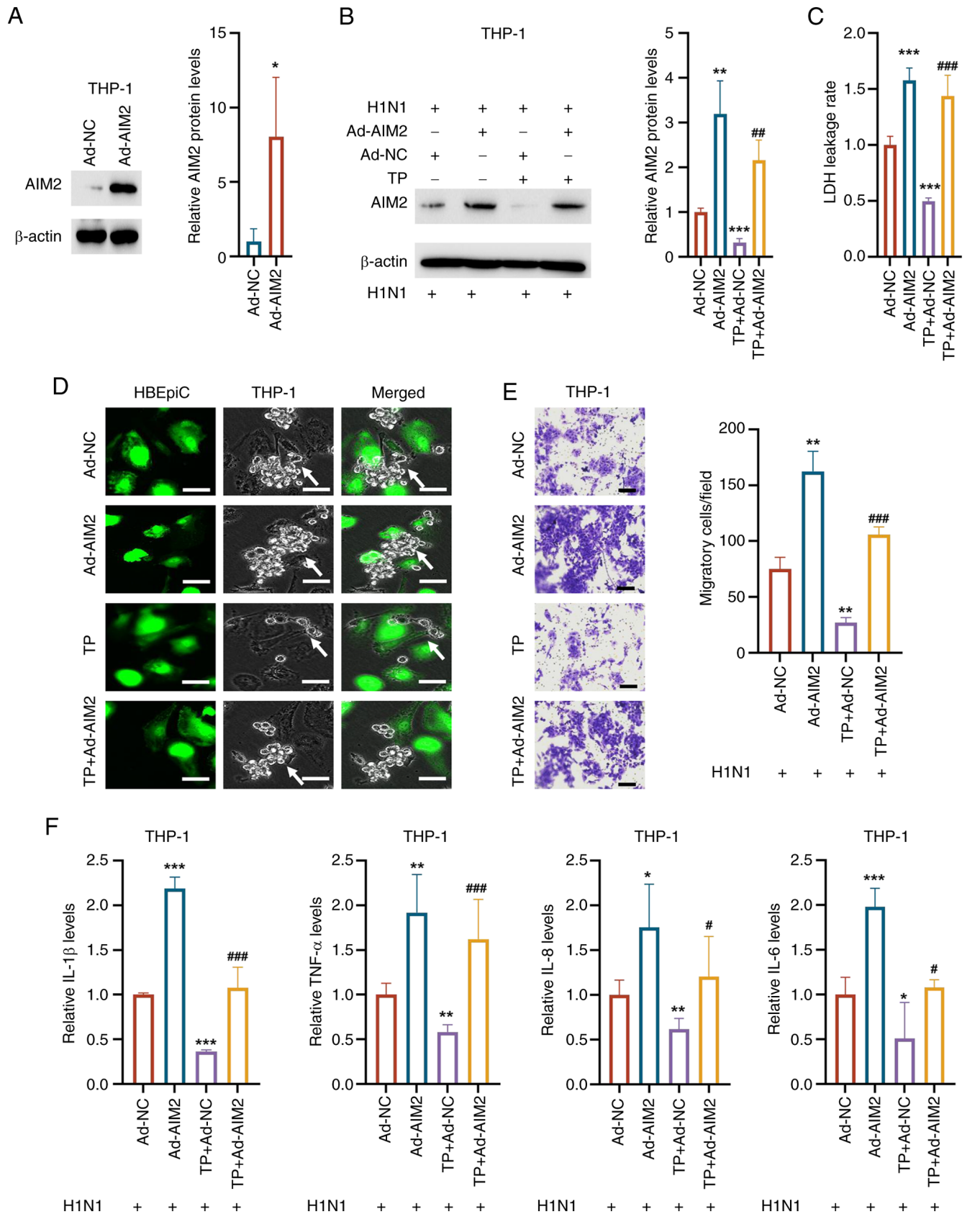

Figure 5. AIM2 overexpression reverses the immunosuppressive effects of TP in THP-1 cells. (A) Transfection with Ad-AIM2 upregulated the expression of AIM2 compared with that of Ad-NC in THP-1 cells. (B) AIM2 protein levels were elevated in THP-1 cells overexpressing AIM2 compared with control THP-1 cells. (C) In THP-1 cells, AIM2 overexpression increased the LDH leakage rate. (D) AIM2 overexpression reversed the TP-induced reduction in adhesion between THP-1 cells and HBEpiCs (scale bar, 10 μm). (E) AIM2 overexpression enhanced the migration ability of THP-1 cells compared with that of H1N1-treated control cells and reversed the TP-induced decrease in THP-1 cell migration (scale bar, 50 μm). (F) AIM2 overexpression reversed the TP-induced reduction in inflammatory cytokine levels. The data are presented as the mean ± standard deviation; *P<0.05, **P<0.01, ***P<0.001 vs. Con; $^{\#}$P<0.05, $^{\#\#}$P<0.01, $^{\#\#\#}$P<0.001 vs. Ad-AIM2. AIM2, absent in melanoma 2; TP, triptolide; LDH, lactate dehydrogenase; HBEpiCs, human bronchial epithelial cells; H1N1, influenza A; GSDMD, gasdermin D; IL, interleukin; TNF-α, tumor necrosis factor-α; Con, control.

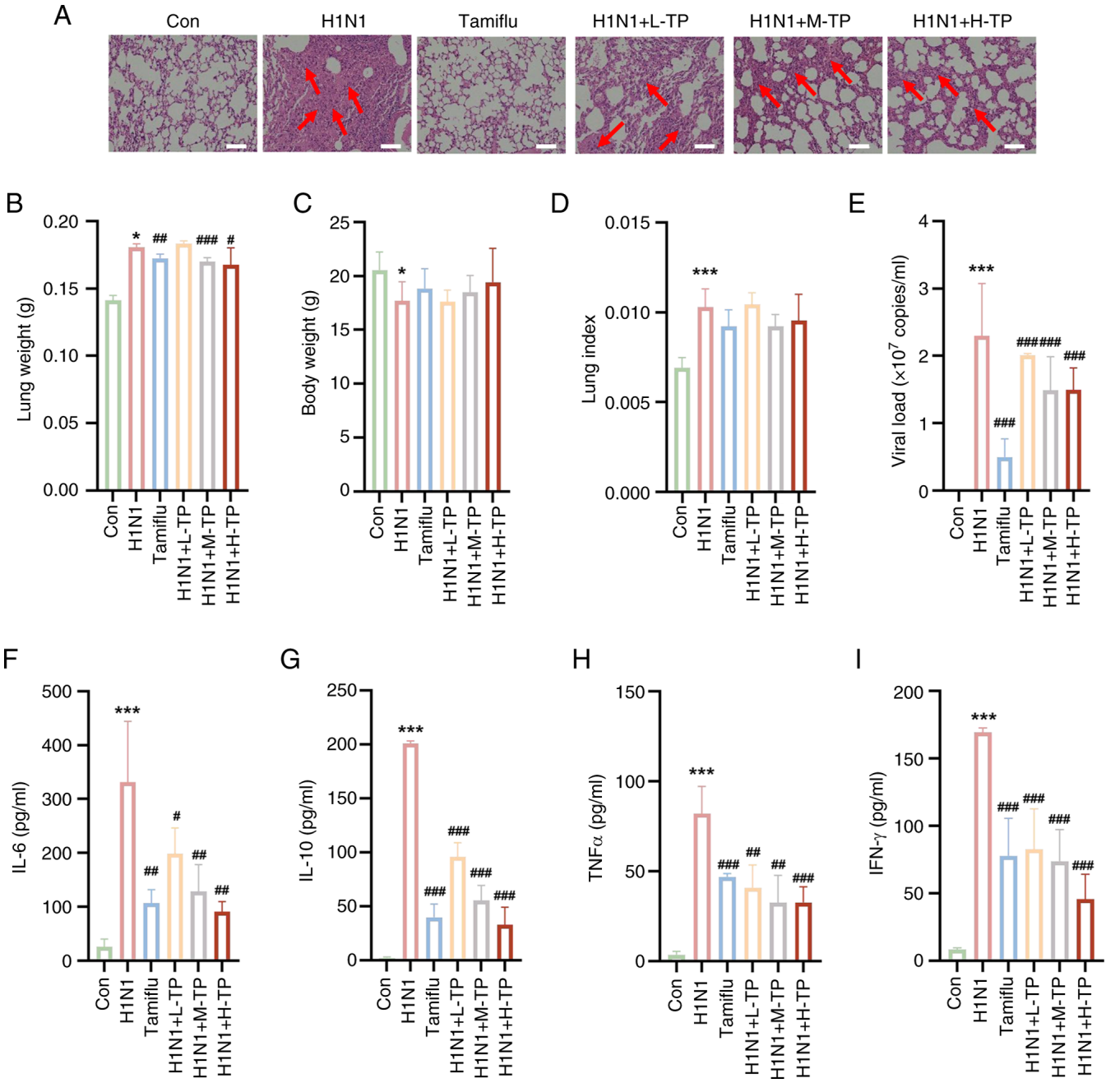

Figure 6. TP modulates the immune response and alleviates lung injury in a murine H1N1 pneumonia model. (A) Representative images of hematoxylin and eosin stained sections (magnification, x20; red arrows demarcate regions of pulmonary consolidation; scale bar, 100 μm). (B) H1N1 infection led to increased lung weight compared with that in the control group, whereas lung weight was markedly reduced in the Tamiflu, L-TP, M-TP, and H-TP groups. (C) No significant changes in body weight were observed among the treatment groups. (D) The lung index was decreased in the H1N1 group and did not fully recover in the four treatment groups. (E) The Tamiflu, L-TP, M-TP, and H-TP treatment groups presented markedly reduced viral loads compared with the H1N1 group, with the Tamiflu group exhibiting the most significant reduction. (F-I) Following H1N1 infection, inflammatory cytokine levels were elevated, but treatment with Tamiflu, L-TP, M-TP, and H-TP markedly reduced these levels in a dose-dependent manner. The data are expressed as the mean ± standard deviation; *P<0.05, **P<0.01, ***P<0.001, vs. Con; $^{\#}$P<0.05, $^{\#\#}$P<0.01, $^{\#\#\#}$P<0.001 vs. H1N1; $^{\$\$}$P<0.01 vs. H1N1+L-TP. TP, triptolide; H1N1, influenza A; Con, control.

antiviral effects (16,34). Unlike Tamiflu, TP not only acts as an antiviral drug but also offers unique advantages in immune modulation and inflammation control. Therefore, the combined use of Tamiflu and TP could provide a more comprehensive treatment approach for H1N1-induced pneumonia, especially for critically ill patients, and warrants further investigation.

Pathophysiological mechanisms of H1N1-induced pneumonia. H1N1 infection activates the interaction between alveolar epithelial cells and immune cells, triggering a series of immune responses that ultimately lead to the development of pneumonia (35). Initially, the H1N1 virus infects alveolar epithelial cells, which recognize the virus through pattern recognition receptors (such as Toll-like receptors) and activate an immune response, releasing a number of proinflammatory cytokines, including IL-6, IL-8 and TNF-α (35). These cytokines recruit immune cells, such as neutrophils and macrophages, to the site of infection (36). In addition, infected alveolar epithelial

cells secrete alert factors that activate immune cells such as dendritic cells and macrophages, which further amplify the inflammatory response (36). These immune cells also release interferons to inhibit viral replication but may exacerbate local inflammation (37). As immune cells are overactivated, a cytokine storm occurs, and the release of cytokines (such as IL-1β, IL-6 and TNF-α) increases vascular permeability, leading to the infiltration of more immune cells into the lung tissue, thereby triggering a more severe inflammatory response and tissue damage (38). This excessive immune response and local tissue damage not only destroy alveolar epithelial cells and endothelial cells but also lead to fluid accumulation in the lungs, impairing normal gas exchange, which ultimately leads to ARDS and progresses to pneumonia (39). Prolonged inflammation and immune cell infiltration may further result in pulmonary fibrosis, severely impairing lung function. This series of processes collectively contributes to the development of severe pneumonia and respiratory failure caused by H1N1 infection (39,40). Consistent with these findings, after H1N1 infection, the levels of inflammatory factors in THP1 cells and HBEpiCs cultured *in vitro* increased in the present study. Furthermore, the adhesion between these two cell types and the migration capacity of the THP-1 cells increased. Increased cell adhesion and migration may represent a response of the immune system to combat viral invasion. The increased chemotaxis of immune cells helps direct more immune cells to the site of infection, increasing local immune responses to counter the spread of the virus.

Cell type-specific activation of AIM2 inflammasome in H1N1 immunopathology. During the immune response to H1N1 infection, AIM2 recognizes viral RNA or DNA to activate immune cells, particularly macrophages and dendritic cells, initiating the host antiviral immune response (41). However, when the activation of AIM2 is excessive, it may exacerbate the inflammatory response and lead to severe lung damage (41,42). Overactivation of AIM2 not only induces the release of proinflammatory cytokines, such as IL-1β and IL-18, but may also trigger a cytokine storm, further intensifying local inflammation (43). This excessive immune response results in lung tissue damage, disruption of the alveolar structure and impairment of gas exchange function (43). AIM2 activates caspase-1 to trigger the formation of the inflammasome, which facilitates the maturation and secretion of IL-1β and IL-18 (44). In this process, the activation of caspase-1 is critical for the expansion of the inflammatory response, as it not only participates in the activation of proinflammatory cytokines but also cleaves GSDMD protein, leading to the formation of GSDMD pores (45). GSDMD is a membrane-penetrating protein that forms pores in the cell membrane, resulting in cell rupture and the release of additional proinflammatory factors, thus exacerbating the immune response and causing local tissue damage (45). Overactivation of AIM2, caspase-1, and GSDMD plays a crucial role in the development of pneumonia induced by H1N1 infection. First, the interactions between these molecules lead to the occurrence of a cytokine storm, particularly in severe H1N1 infections (46). The cytokine storm increases vascular permeability and causes extensive immune cell infiltration into lung tissue, worsening lung damage and potentially leading to life-threatening complications such as acute respiratory failure. Second, sustained inflammation can result in chronic lung tissue damage, including destruction of alveolar structures and disruption of gas exchange, eventually leading to lung fibrosis and further impairment of lung function. Therefore, the overactivation of AIM2, caspase-1, and GSDMD in H1N1-induced pneumonia contributes to the severity of pneumonia through excessive immune responses and cell death, complicating treatment. In the present study, H1N1 infection activated AIM2 signaling in THP-1 cells, whereas AIM2 signaling in HBEpiCs remained unchanged. These findings suggested that the activation of AIM2 in immune cells could be a critical mechanism underlying H1N1-induced pneumonia, with excessive immune activation potentially leading to aggravated inflammation and tissue damage.

Dual antiviral and immunomodulatory roles of TP. An increasing number of studies have demonstrated that TP has significant antiviral effects. For example, TP inhibits the replication of HSV-1 in a dose-dependent manner without showing cytotoxicity, suggesting that its action may involve specific cellular components rather than broad toxicity (47). Moreover, TP has been shown to enhance the oncolytic activity of vesicular stomatitis virus by suppressing antiviral immune responses, thereby delaying tumor growth and prolonging survival in mouse models (47). The present study investigated whether TP could ameliorate pneumonia induced by the H1N1 influenza virus. *In vitro* and *in vivo* experiments both confirmed that TP effectively reduced inflammatory responses in alveolar epithelial cells and immune cells. Additionally, *in vivo* studies revealed that TP partially inhibited the transcription of the H1N1 virus. These findings validated the potent antiviral and anti-inflammatory properties of TP. Notably, TP demonstrated low cytotoxicity under the tested conditions especially in alveolar epithelial cells, since treating HBEpiCs with TP at concentrations of 5, 10 and 20 nM did not markedly affect cell viability compared with the control. However, TP did have some cytotoxic effects on immune cells, such as THP-1 cells, which suggested that its immune-modulating effects might involve a trade-off in immune cell viability. This finding warrants further investigation into the optimal dosing of TP for therapeutic use, ensuring that its beneficial antiviral and anti-inflammatory effects are maximized while minimizing toxicity to immune cells.

Next, the present study explored the regulatory effects of TP on the AIM2 signaling pathway in HBEpiCs and THP-1 cells. The results showed that TP treatment did not markedly alter the AIM2 signaling pathway in HBEpiCs. This may reflect the fact that HBEpiCs maintain stable AIM2 signal activation, primarily exerting their antiviral effects rather than modulating the inflammatory response to mediate cell damage (48). By contrast, TP exerted a significant inhibitory effect in THP-1 cells, as evidenced by decreased mRNA and protein expression of AIM2 and reduced formation of ASC-AIM2 complexes. Excessive activation of the AIM2 signaling pathway often leads to an overreaction of immune cells, resulting in the excessive release of inflammatory factors (such as IL-1β, IL-6, and TNF-α) (49). Thus, TP reversed the inflammatory response in THP-1 cells by suppressing the AIM2 signaling pathway.

Further experiments demonstrated that TP not only reduced the levels of inflammatory factors in THP-1 cells but also attenuated the overactivation of immune cells and suppressed the excessive inflammatory response induced by these cells. Importantly, when AIM2 was overexpressed in THP-1 cells, the regulatory effects of TP on inflammatory factors and other indicators were markedly blocked, suggesting that the suppression of AIM2 signaling is a key mechanism of action of TP. In summary, TP alleviates the inflammatory burden in HBEpiCs by inhibiting AIM2 signaling in THP-1 cells.

Study limitations and future directions. There are several limitations to the present study that warrant consideration. First, the *in vitro* experiments used HBEpiC and THP-1 cell lines to model airway epithelial and immune responses, respectively. While these cell lines are valuable for controlled studies, they may not fully replicate the complexity of primary human cells or the *in vivo* environment. Second, the *in vivo* assessments employed a murine model of H1N1-induced pneumonia to evaluate the effects of TP. However, differences between murine and human immune systems, including variations in cytokine profiles and immune cell populations, may limit the direct applicability of these findings to human physiology. Building upon these findings, future research directions should include the incorporation of more complex models, such as human organoids or nonhuman primate models, to improve the simulation of human responses and evaluate the efficacy and safety of TP in settings that more closely resemble human physiology. Moreover, the present study did not delineate the specific molecular pathways through which TP exerts its antiviral effects on H1N1. Although TP showed efficacy in inhibiting viral replication, the exact targets and mechanisms, such as potential interference with viral RNA synthesis or modulation of the host cell translation machinery, were not directly investigated in the present study. To build upon the findings of the present study, future studies should aim to elucidate the molecular mechanisms by which TP inhibits H1N1 replication. This includes investigating whether TP directly affects viral RNA polymerase activity, impedes the assembly of viral ribonucleoprotein complexes, or modulates host factors involved in viral replication and protein synthesis. Understanding these mechanisms will provide deeper insights into the antiviral properties of TP and support its potential development as a therapeutic agent against influenza.

Based on its findings, the present study demonstrated that TP selectively modulated the AIM2 signaling pathway in immune cells, abolishing excessive activation of macrophages and neutrophils while preserving alveolar epithelial cell viability. This cell type-specific targeting markedly reduced pathogenic immune cell-epithelial cell interactions, thereby alleviating H1N1-induced lung immunopathology. Crucially, the dual capacity of TP to suppress viral replication and mitigate immune system dysregulation provides a novel therapeutic strategy for severe viral pneumonia. As a selective immune modulator, it may synergize with existing antivirals to bridge the critical gap between viral clearance and inflammation control, thereby ultimately minimizing organ damage in high-risk patients.

Acknowledgements

Not applicable.

Funding

The present study was funded by the National Natural Science Foundation of China (grant no. 82405094), the Shenzhen Natural Science Foundation (grant no. JCYJ20240813152345060) and the Science and Technology Planning Project of Shenzen Municipality (grant no. JSGG20220226090203006).

Availability of data and materials

The data generated in the present study may be requested from the corresponding author.

Authors' contributions

YC, HW, and XW performed the experiments and wrote the paper. LC performed the experiments and interpreted the data. XF, RQ, DJ, ML and WX performed part of the animal experiments. WZ supervised the project, interpreted the data and wrote the paper. All authors confirm the authenticity of all the raw data. All authors read and approved the final manuscript.

Ethics approval and consent to participate

All the experimental procedures for the mice were performed in accordance with the guidelines of the Institutional Animal Care and Use Committee. The protocol was approved by the Committee on the Ethics of Animal Experiments of Guangzhou University of Chinese Medicine (approval no. 2024055R).

Patient consent for publication

Not applicable.

Competing interests

The authors declare that they have no competing interests.

References

1. Li X, Gu M, Zheng Q, Gao R and Liu X: Packaging signal of influenza A virus. Virol J 18: 36, 2021.
2. Dong Y, Wang L, Burgner DP, Miller JE, Song Y, Ren X, Li Z, Xing Y, Ma J, Sawyer SM and Patton GC: Infectious diseases in children and adolescents in China: Analysis of national surveillance data from 2008 to 2017. BMJ 369: m1043, 2020.
3. Chen Z, Tsui JL, Cai J, Su S, Viboud C, du Plessis L, Lemey P, Kraemer MUG and Yu H: Disruption of seasonal influenza circulation and evolution during the 2009 H1N1 and COVID-19 pandemics in Southeastern Asia. Nat Commun 16: 475, 2025.
4. Ghorbani A, Ngunjiri JM and Lee CW: Influenza A virus subpopulations and their implication in pathogenesis and vaccine development. Annu Rev Anim Biosci 8: 247-267, 2020.
5. Park J, Fong Legaspi SL, Schwartzman LM, Gygli SM, Sheng ZM, Freeman AD, Matthews LM, Xiao Y, Ramuta MD, Batchenkova NA, *et al*: An inactivated multivalent influenza A virus vaccine is broadly protective in mice and ferrets. Sci Transl Med 14: eabo2167, 2022.

6. Pinto RM, Bakshi S, Lytras S, Zakaria MK, Swingler S, Worrell JC, Herder V, Hargrave KE, Varjak M, Cameron-Ruiz N, *et al*: BTN3A3 evasion promotes the zoonotic potential of influenza A viruses. Nature 619: 338-347, 2023.
7. Huang L, Wang J, Ma X, Sun L, Hao C and Wang W: Inhibition of influenza a virus infection by natural stilbene piceatannol targeting virus hemagglutinin. Phytomedicine 120: 155058, 2023.
8. Yu J, Li H, Jia J, Huang Z, Liu S, Zheng Y, Mu S, Deng X, Zou X, Wang Y, *et al*: Pandemic influenza A (H1N1) virus causes abortive infection of primary human T cells. Emerg Microbes Infect 11: 1191-1204, 2022.
9. Zheng Y, He D, Zuo W, Wang W, Wu K, Wu H, Yuan Y, Huang Y, Li H, Lu Y, *et al*: Influenza A virus dissemination and infection leads to tissue resident cell injury and dysfunction in viral sepsis. EBioMedicine 116: 105738, 2025.
10. Meng X, Zhu Y, Yang W, Zhang J, Jin W, Tian R, Yang Z and Wang R: HIF-1α promotes virus replication and cytokine storm in H1N1 virus-induced severe pneumonia through cellular metabolic reprogramming. Virol Sin 39: 81-96, 2024.
11. Rewar S, Mirdha D and Rewar P: Treatment and prevention of pandemic H1N1 influenza. Ann Glob Health 81: 645-653, 2015.
12. Lampejo T: Influenza and antiviral resistance: An overview. Eur J Clin Microbiol Infect Dis 39: 1201-1208, 2020.
13. Xu DW and Tate MD: Taking AIM at influenza: The role of the AIM2 inflammasome. Viruses 16: 1535, 2024.
14. Zhang H, Luo J, Alcorn JF, Chen K, Fan S, Pilewski J, Liu A, Chen W, Kolls JK and Wang J: AIM2 inflammasome is critical for influenza-induced lung injury and mortality. J Immunol 198: 4383-4393, 2017.
15. Schattgen SA, Gao G, Kurt-Jones EA and Fitzgerald KA: Cutting edge: DNA in the lung microenvironment during influenza virus infection tempers inflammation by engaging the DNA sensor AIM2. J Immunol 196: 29-33, 2016.
16. Gao J, Zhang Y, Liu X, Wu X, Huang L and Gao W: Triptolide: Pharmacological spectrum, biosynthesis, chemical synthesis and derivatives. Theranostics 11: 7199-7221, 2021.
17. Fang WY, Tseng YT, Lee TY, Fu YC, Chang WH, Lo WW, Lin CL and Lo YC: Triptolide prevents LPS-induced skeletal muscle atrophy via inhibiting NF-κB/TNF-α and regulating protein synthesis/degradation pathway. Br J Pharmacol 178: 2998-3016, 2021.
18. Han R, Rostami-Yazdi M, Gerdes S and Mrowietz U: Triptolide in the treatment of psoriasis and other immune-mediated inflammatory diseases. Br J Clin Pharmacol 74: 424-436, 2012.
19. Wang N, Min X, Ma N, Zhu Z, Cao B, Wang Y, Yong Q, Huang J and Li K: The negative impact of triptolide on the immune function of human natural killer cells. Pharmaceuticals (Basel) 16: 458, 2023.
20. Zhu W, Li Y, Zhao J, Wang Y, Li Y and Wang Y: The mechanism of triptolide in the treatment of connective tissue disease-related interstitial lung disease based on network pharmacology and molecular docking. Ann Med 54: 541-552, 2022.
21. Liu C, Wu X, Bing X, Qi W, Zhu F, Guo N, Li C, Gao X, Cao X, Zhao M and Xia M: H1N1 influenza virus infection through NRF2-KEAP1-GCLC pathway induces ferroptosis in nasal mucosal epithelial cells. Free Radic Biol Med 204: 226-242, 2023.
22. Wei Z, Gao R, Sun Z, Yang W, He Q, Wang C, Zhang J, Zhang X, Guo L and Wang S: Baicalin inhibits influenza A (H1N1)-induced pyroptosis of lung alveolar epithelial cells via caspase-3/GSDME pathway. J Med Virol 95: e28790, 2023.
23. Livak KJ and Schmittgen TD: Analysis of relative gene expression data using real-time quantitative PCR and the 2(-Delta Delta C(T)) method. Methods 25: 402-408, 2001.
24. Du HX, Zhou HF, Yang JH, Lu YY, He Y and Wan HT: Preliminary study of Yinhuapinggan granule against H1N1 influenza virus infection in mice through inhibition of apoptosis. Pharm Biol 58: 979-991, 2020.
25. Paukner S, Kimber S, Cumper C, Rea-Davies T, Sueiro Ballesteros L, Kirkham C, Hargreaves A, Gelone SP, Richards C and Wicha WW: In vivo immune-modulatory activity of lefamulin in an influenza virus A (H1N1) infection model in mice. Int J Mol Sci 25: 5401, 2024.
26. Wan YS, You Y, Ding QY, Xu YX, Chen H, Wang RR, Huang YW, Chen Z, Hu WW and Jiang L: Triptolide protects against white matter injury induced by chronic cerebral hypoperfusion in mice. Acta Pharmacol Sin 43: 15-25, 2022.
27. Zeldin DC, Wohlford-Lenane C, Chulada P, Bradbury JA, Scarborough PE, Roggli V, Langenbach R and Schwartz DA: Airway inflammation and responsiveness in prostaglandin H synthase-deficient mice exposed to bacterial lipopolysaccharide. Am J Respir Cell Mol Biol 25: 457-465, 2001.
28. Matute-Bello G, Downey G, Moore BB, Groshong SD, Matthay MA, Slutsky AS and Kuebler WM; Acute Lung Injury in Animals Study Group: An official American thoracic society workshop report: Features and measurements of experimental acute lung injury in animals. Am J Respir Cell Mol Biol 44: 725-738, 2011.
29. Gao J, Peng S, Shan X, Deng G, Shen L, Sun J, Jiang C, Yang X, Chang Z, Sun X, *et al*: Inhibition of AIM2 inflammasome-mediated pyroptosis by Andrographolide contributes to amelioration of radiation-induced lung inflammation and fibrosis. Cell Death Dis 10: 957, 2019.
30. Zhou J, Li S, Yang Y, Zhou C, Wang C and Zeng Z: Triptolide alleviates acute lung injury by reducing mitochondrial dysfunction mediated ferroptosis through the STAT3/p53 pathway. Free Radic Biol Med 230: 79-94, 2025.
31. Yoo ES: Study of specific oligosaccharide structures related with swine flu (H1N1) and avian flu, and tamiflu as their remedy. J Microbiol Biotechnol 21: 449-454, 2011.
32. Zima V, Albiñana CB, Rojíková K, Pokorná J, Pachl P, Řezáčová P, Hudlicky J, Navrátil V, Majer P, Konvalinka J, *et al*: Investigation of flexibility of neuraminidase 150-loop using tamiflu derivatives in influenza A viruses H1N1 and H5N1. Bioorg Med Chem 27: 2935-2947, 2019.
33. Gu C, Chen Y, Li H, Wang J and Liu S: Considerations when treating influenza infections with oseltamivir. Expert Opin Pharmacother 25: 1301-1316, 2024.
34. Hou W, Liu B and Xu H: Triptolide: Medicinal chemistry, chemical biology and clinical progress. Eur J Med Chem 176: 378-392, 2019.
35. Ling L, Ren A, Lu Y, Zhang Y, Zhu H, Tu P, Li H and Chen D: The synergistic effect and mechanisms of flavonoids and polysaccharides from Houttuynia cordata on H1N1-induced pneumonia in mice. J Ethnopharmacol 302: 115761, 2023.
36. Fontes CA, Dos Santos AAS and De Oliveira SA: High-resolution computed tomography enhances the diagnosis and follow-up of influenza A (H1N1) virus-associated pneumonia. J Infect Dev Ctries 14: 317-320, 2020.
37. Himaal Dev GJ, Venkategowda PM, Sutar AR and Shankar V: Intestinal mucormycosis in an adult with H1N1 pneumonia on extracorporeal membrane oxygenation. Ann Card Anaesth 24: 92-94, 2021.
38. Ding W, Li R, Song T, Yang Z, Xu D, Huang C, Shen S, Zhong N, Lai K and Deng Z: AMG487 alleviates influenza A (H1N1) virus-induced pulmonary inflammation through decreasing IFN-γ-producing lymphocytes and IFN-γ concentrations. Br J Pharmacol 181: 2053-2069, 2024.
39. Zhang S, Sun F, Zhu J, Qi J, Wang W, Liu Z, Li W, Liu C, Liu X, Wang N, *et al*: Phillyrin ameliorates influenza a virus-induced pulmonary inflammation by antagonizing CXCR2 and inhibiting NLRP3 inflammasome activation. Virol J 20: 262, 2023.
40. Arranz-Herrero J, Presa J, Rius-Rocabert S, Utrero-Rico A, Arranz-Arija JA, Lalueza A, Escribese MM, Ochando J, Soriano V and Nistal-Villan E: Determinants of poor clinical outcome in patients with influenza pneumonia: A systematic review and meta-analysis. Int J Infect Dis 131: 173-179, 2023.
41. Han Y, Ge C, Ye J, Li R and Zhang Y: Demethyleneberberine alleviates Pseudomonas aeruginosa-induced acute pneumonia by inhibiting the AIM2 inflammasome and oxidative stress. Pulm Pharmacol Ther 83: 102259, 2023.
42. Tseng YH, Chen IC, Li WC and Hsu JH: Regulatory cues in pulmonary fibrosis-with emphasis on the AIM2 inflammasome. Int J Mol Sci 24: 10876, 2023.
43. Cho SJ, Hong KS, Jeong JH, Lee M, Choi AMK, Stout-Delgado HW and Moon JS: DROSHA-dependent AIM2 inflammasome activation contributes to lung inflammation during idiopathic pulmonary fibrosis. Cells 8: 938, 2019.
44. Cho SJ, Moon JS, Nikahira K, Yun HS, Harris R, Hong KS, Huang H, Choi AMK and Stout-Delgado H: GLUT1-dependent glycolysis regulates exacerbation of fibrosis via AIM2 inflammasome activation. Thorax 75: 227-236, 2020.
45. Zhang T, Du H, Feng S, Wu R, Chen T, Jiang J, Peng Y, Ye C and Fang R: NLRP3/ASC/caspase-1 axis and serine protease activity are involved in neutrophil IL-1β processing during Streptococcus pneumoniae infection. Biochem Biophys Res Commun 513: 675-680, 2019.

46. Fang R, Tsuchiya K, Kawamura I, Shen Y, Hara H, Sakai S, Yamamoto T, Fernandes-Alnemri T, Yang R, Hernandez-Cuellar E, *et al*: Critical roles of ASC inflammasomes in caspase-1 activation and host innate resistance to Streptococcus pneumoniae infection. J Immunol 187: 4890-4899, 2011.
47. Aliabadi N, Jamalidoust M, Pouladfar G, Ziyaeyan A and Ziyaeyan M: Antiviral activity of triptolide on herpes simplex virus in vitro. Immun Inflamm Dis 10: e667, 2022.
48. Ben Yebdri F, Van Grevenynghe J, Tang VA, Goulet ML, Wu JH, Stojdl DF, Hiscott J and Lin R: Triptolide-mediated inhibition of interferon signaling enhances vesicular stomatitis virus-based oncolysis. Mol Ther 21: 2043-2053, 2013.
49. Tian J, Liu Y, Gao W, Shi X, Cheng F and Xie B: NETs activate AIM2 to mediate synovial fibroblast pyroptosis and promote acute gouty arthritis development. Immunol Lett 275: 107007, 2025.